Chapter 2
Planar Curves Whose Curvature Depends Only on the Distance From a Fixed Point

Abstract Looking at the Frenet-Serret equations from the viewpoint of dynamical systems, one can prove that when the curvature of a plane curve is given as a function of the radius, the problem of reconstructing this curve is reducible to quadratures. Additionally, two different integration procedures are presented. These methods are illustrated first via the famous lemniscate of Bernoulli, which is immediately related to the Euler elastica. Relying on the new formalism, the Sturm spirals and their generalizations, the Serret curves (which have a mechanical origin) and their generalizations are parametrized explicitly. The results on the Serret curves are original, as their description up to now has been purely abstract. Finally, the same technique is applied to the Cassinian ovals, and in this way, one concludes with their alternative parameterizations.

2.1 The Moving Frame Associated with a Plane Curve

The fundamental existence and uniqueness theorem in the theory of plane curves states that a curve is uniquely determined (up to Euclidean motion) by its curvature given as a function of its arc-length (see Berger and Gostiaux (1988), p. 296 or Oprea (2007), p. 37). The simplicity of the situation, however, is elusive, as in many cases, it is impossible to find the curve explicitly. Having that in mind, it is clear that if the curvature is given as a function of its position, the situation is even more complicated. Viewing the Frenet-Serret equations as a fictitious dynamical system, it was proven in Vassilev et al. (2009) (see also Djondjorov et al. (2009a)) that when the curvature is given simply as a function of the distance from the origin, the problem can always be reduced to quadratures. This last result is not entirely new, as Singer (1999) had already shown that in some cases, it is possible that such a curvature has an interpretation as a central potential in the plane, and therefore the trajectories can be found through the standard procedures in classical mechanics. However, the approach which we will follow here is entirely different from the group-theoretical approach of Vassilev et al. (2009) or the mechanical approach of Singer (1999) proposed in those papers. The method is illustrated by the most natural example in the class of curves whose curvatures are functions only of the distance from the

I.M. Mladenov and M. Hadzhilazova, *The Many Faces of Elastica*,
Forum for Interdisciplinary Mathematics 3, DOI 10.1007/978-3-319-61244-7_2

origin. Here, we consider in some detail the cases in which the function in question is either proportional or inversely proportional to the distance from the origin. Let us start with the first case, namely,

$$\kappa = \sigma r, \qquad r = |\mathbf{x}| = \sqrt{x^2 + z^2}, \tag{2.1}$$

where x, z are the Cartesian coordinates in the plane XOZ, which have to be considered as functions of the arc-length parameter s, and σ is assumed to be a positive real constant.

If $\theta(s)$ denotes the slope of the tangent to the curve with respect to the OX axis, one has the following geometrical relations:

$$\frac{\mathrm{d}\theta(s)}{\mathrm{d}s} = \kappa(s), \qquad \frac{\mathrm{d}x}{\mathrm{d}s} = \cos\theta(s), \qquad \frac{\mathrm{d}z}{\mathrm{d}s} = \sin\theta(s), \tag{2.2}$$

which can also be deduced from the Frenet-Serret equations (see also Fig. 1.1)

$$\frac{\mathrm{d}\mathbf{x}(s)}{\mathrm{d}s} = \mathbf{T}(s), \qquad \frac{\mathrm{d}\mathbf{T}}{\mathrm{d}s} = \kappa\mathbf{N}, \qquad \frac{\mathrm{d}\mathbf{N}}{\mathrm{d}s} = -\kappa\mathbf{T}, \tag{2.3}$$

where $\mathbf{T}$ and $\mathbf{N}$ are, respectively, the tangent and the normal vectors to the curve, and s is the natural parameter along it. Combining (2.1) and (2.2), we get

$$\frac{\mathrm{d}\theta(s)}{\mathrm{d}s} = \kappa(r), \tag{2.4}$$

which is still quite an unpromising equation. We will proceed (as suggested but not pursued in Singer (1999)) by going to the co-moving frame $(\mathbf{T}, \mathbf{N})$ associated with the curve

$$\mathbf{x} = \xi\mathbf{T} + \eta\mathbf{N} \tag{2.5}$$

accordingly, the Frenet-Serret equations (2.3) take the form

$$\frac{\mathrm{d}\xi}{\mathrm{d}s} = \dot{\xi} = \kappa\eta + 1, \qquad \frac{\mathrm{d}\eta}{\mathrm{d}s} = \dot{\eta} = -\kappa\xi. \tag{2.6}$$

2.2 Integration

Multiplying the first equation in (2.6) by ξ, the second one by η, and summing up the so-obtained expressions, we find that

$$\xi = r\dot{r}, \tag{2.7}$$

in which the dot means a differentiation with respect to the arc-length parameter. Substituting this expression back into the second equation of (2.6) and integrating, we obtain

$$\eta = -\int \kappa(r) r \mathrm{d}r + c, \tag{2.8}$$

where c is the integration constant. One should notice, however (cf. equation (2.5)), that the coordinates in the moving frame are not entirely independent, but rather obey the constraint

$$\xi^2 + \eta^2 = r^2, \tag{2.9}$$

which, in view of Eqs. (2.7) and (2.8), presents an ordinary differential equation for the radial coordinate r.

2.3 Bernoulli's Lemniscates

This curve is a special case (when $a \equiv c$) of the Cassinian ovals (see Mladenov (2000) and the end of this chapter), defined by the equation

$$(x^2 + z^2)^2 - 2a^2(z^2 - x^2) + a^4 - c^4 = 0, \tag{2.10}$$

and has a curvature (which can be found using formula (1.18)) that is linear in r. Inserting $\kappa = \sigma r$ into Eq. (2.8) produces

$$\eta = -\frac{\sigma r^3}{3} \tag{2.11}$$

(the integration constant is taken to be zero) and the scheme from the previous section leads to the equation

$$\frac{\mathrm{d}r}{\mathrm{d}s} = \sqrt{1 - \frac{\sigma^2 r^4}{9}}\,. \tag{2.12}$$

Its integration is immediate and gives us

$$r = \sqrt{\frac{3}{\sigma}}\,\mathrm{cn}\left(\sqrt{\frac{2\sigma}{3}}s, \frac{1}{\sqrt{2}}\right), \tag{2.13}$$

where $\mathrm{cn}(u, k)$ denotes one of the Jacobian elliptic functions in which the first slot is occupied by its argument and the second one by the so-called elliptic modulus (a real number between zero and one). More details about elliptic functions and integrals can be found in Jahnke et al. (1960) and Olver et al. (2010). Substituting this solution into Eqs. (2.7) and (2.8) has, as a result, the coordinates of the lemniscate in the moving frame

$$\xi = -\sqrt{\frac{6}{\sigma}}\,\mathrm{cn}\Big(\sqrt{\frac{2\sigma}{3}}s,\,\frac{1}{\sqrt{2}}\Big)\mathrm{dn}\Big(\sqrt{\frac{2\sigma}{3}}s,\,\frac{1}{\sqrt{2}}\Big)\mathrm{sn}\Big(\sqrt{\frac{2\sigma}{3}}s,\,\frac{1}{\sqrt{2}}\Big)$$
$$\eta = -\sqrt{\frac{3}{\sigma}}\,\mathrm{cn}^3\Big(\sqrt{\frac{2\sigma}{3}}s,\,\frac{1}{\sqrt{2}}\Big). \tag{2.14}$$

With respect to the fixed one, these functions give a new curve which we will call the co-lemniscate. Written in terms of its components, Eq. (2.5) tells us that the lemniscate coordinates x, z are obtained from those of the co-lemniscate ξ, η via a plane rotation specified by the slope angle θ, i.e.,

$$x = \xi\cos\theta - \eta\sin\theta, \qquad z = \xi\sin\theta + \eta\cos\theta. \tag{2.15}$$

Obviously, what remains to be done is to find θ, and this can be achieved via an integration of the first equation in (2.2). In this way, we obtain

$$\theta = 3\arccos\Big(\mathrm{dn}\Big(\sqrt{\frac{2\sigma}{3}}s,\,\frac{1}{\sqrt{2}}\Big)\Big)$$
$$= 3\arcsin\Big(\tilde{k}\,\mathrm{sn}\Big(\sqrt{\frac{2\sigma}{3}}s,\,\frac{1}{\sqrt{2}}\Big)\Big), \qquad \tilde{k} = \sqrt{1-k^2}. \tag{2.16}$$

Now we have to take into account the trigonometric identities

$$\sin 3\varphi = 3\sin\varphi - 4\sin^3\varphi, \qquad \cos 3\varphi = 4\cos^3\varphi - 3\cos\varphi, \tag{2.17}$$

which give us

$$\sin\theta = \frac{3}{\sqrt{2}}\mathrm{sn}\Big(\sqrt{\frac{2\sigma}{3}}s,\,\frac{1}{\sqrt{2}}\Big) - \sqrt{2}\,\mathrm{sn}^3\Big(\sqrt{\frac{2\sigma}{3}}s,\,\frac{1}{\sqrt{2}}\Big)$$
$$\cos\theta = 4\mathrm{dn}^3\Big(\sqrt{\frac{2\sigma}{3}}s,\,\frac{1}{\sqrt{2}}\Big) - 3\mathrm{dn}\Big(\sqrt{\frac{2\sigma}{3}}s,\,\frac{1}{\sqrt{2}}\Big) \tag{2.18}$$

and eventually provide the parameterization of the Bernoullian lemniscate. By making repeated use of the fundamental identities which the Jacobian elliptic functions $\mathrm{sn}(u,k)$, $\mathrm{cn}(u,k)$ and $\mathrm{dn}(u,k)$ satisfy, i.e.,

$$\mathrm{sn}^2(u,k) + \mathrm{cn}^2(u,k) = 1, \qquad \mathrm{dn}^2(u,k) + k^2\,\mathrm{sn}^2(u,k) = 1, \tag{2.19}$$

it is possible to simplify the expressions for x and z into the form

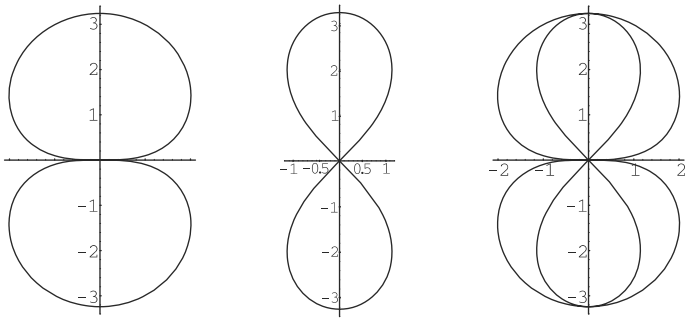

Fig. 2.1 The Bernoullian co-lemniscate (*left*), Bernoulli's lemniscate (*middle*) and both of them (*right*) drawn via formulas (2.14) and (2.20) with $\sigma = 3.5$

$$x = \sqrt{\frac{3}{2\sigma}}\,\mathrm{cn}\left(\sqrt{\frac{2\sigma}{3}}s, \frac{1}{\sqrt{2}}\right)\mathrm{sn}\left(\sqrt{\frac{2\sigma}{3}}s, \frac{1}{\sqrt{2}}\right)$$
$$z = -\sqrt{\frac{3}{\sigma}}\,\mathrm{cn}\left(\sqrt{\frac{2\sigma}{3}}s, \frac{1}{\sqrt{2}}\right)\mathrm{dn}\left(\sqrt{\frac{2\sigma}{3}}s, \frac{1}{\sqrt{2}}\right). \tag{2.20}$$

The properties of the Jacobian functions also make obvious the relations

$$\eta^2 = \left(\frac{\sigma}{3}\right)^2 (\xi^2 + \eta^2)^3, \qquad z^2 - x^2 = \frac{\sigma}{3}\left(x^2 + z^2\right)^2, \tag{2.21}$$

the last one being simply the standard form of Bernoulli's lemniscate (cf. the equation (2.10)). In polar coordinates $\xi = r\,\cos\psi, \eta = r\,\sin\psi, x = r\,\cos\phi, z = r\,\sin\phi$, the above algebraic curves are of degree six and four, respectively, and take the form

$$\sin\psi = -\frac{\sigma}{3}r^2, \qquad \cos 2\phi = -\frac{\sigma}{3}r^2. \tag{2.22}$$

This remarkable similarity in their polar representations suggests calculation of the curvature of the co-lemniscate. The most convenient method in this situation seems to be the application of the formula

$$\kappa = \frac{|r^2 + 2\dot{r}^2 - r\ddot{r}|}{(r^2 + \dot{r}^2)^{3/2}}, \tag{2.23}$$

in which this time the dots denote differentiations with respect to the polar angle. Through straightforward but tedious calculations, one concludes with the formula

$$\kappa = \frac{2\sigma r\left(\sigma^2 r^4 + 9\right)}{\sqrt{3}\left(\sigma^2 r^4 + 3\right)^{3/2}}. \tag{2.24}$$

Regardless of how similar this curve seems to be to the lemniscate in the polar coordinates, its curvature is quite different from that of the parent curve. Both curves are plotted for illustration in (Fig. 2.1).

Remark Because of the relation between the radial coordinate r and the curvature equation (2.1), we can rewrite Eq. (2.12) in the form

$$\dot{\kappa}^2 + \frac{\kappa^4}{9} = \sigma^2, \tag{2.25}$$

which can be recognized and is referred to further on as the *intrinsic equation* of the Bernoullian lemniscate.

2.4 Relationship Between the Lemniscate and the Elastica

Here, we will outline the relation of Bernoulli's lemniscate to another famous curve invented by Bernoulli, the so-called free (or rectangular) elastica (cf. Djondjorov et al. (2009)), which also appears as a profile curve of the Mylar balloon described in detail in Hadzhilazova and Mladenov (2008) and Mladenov and Oprea (2009).

For this purpose, let us differentiate Eq. (2.25), which gives us

$$\ddot{\kappa}_{\text{lemn}} + \frac{2}{9}\kappa_{\text{lemn}}^3 = 0 \tag{2.26}$$

and presents another form of the intrinsic equation of this interesting curve. By comparing it with the intrinsic equation of the free elastica

$$\ddot{\kappa}_{\text{elas}} + \frac{1}{2}\kappa_{\text{elas}}^3 = 0, \tag{2.27}$$

it is easy to conclude that they are related by the transformation

$$\kappa_{\text{lemn}} = \frac{3}{2}\kappa_{\text{elas}}, \tag{2.28}$$

which has been noticed recently by Matsutani (2010) as well. Actually, the mathematical reason is that the curvature of the Bernoulli elastica is again a linear function of the distance, but this time from the OX axis.

2.5 Spirals

In their article on the subject, Bourbaki have called them the most mysterious curves. Actually, we will not unveil their secrets here, but will simply prove some of their

properties, starting with the fundamental geometrical characteristic that the spirals are just the curves for which the curvature is inversely proportional to the distance from a fixed point in the plane called a pole. In analytical form, this property is expressed via the formula

$$\kappa = \frac{\sigma}{|\mathbf{x}|} = \frac{\sigma}{r} = \frac{\sigma}{\sqrt{x^2 + z^2}}, \qquad \sigma > 0, \tag{2.29}$$

where x, z are the Cartesian coordinates in the plane XOZ, which have to be considered as functions of the arc-length parameter s, and σ is assumed to be a positive real constant. Depending on the numerical value of this constant, we will consider several types of spiral which we will describe in detail.

2.6 Sturmian Spirals

By their very definition (cf. Zwikker (1963)), these plane curves possess the property that at each point, their curvature radius $\mathcal{R}$ coincides with the distance r from the origin. Formulated in curvature terms, this means that their curvature κ is given by formula (2.1), in which $\sigma \equiv 1$. Applying the scheme from Sect. 2.2, one easily finds that

$$\eta = -r + c \tag{2.30}$$

and

$$\dot{r} = \frac{\sqrt{2cr - c^2}}{r}, \qquad c > 0. \tag{2.31}$$

It is convenient to perform the integration of the above equation by switching to a new independent variable t defined by the equation

$$\frac{\mathrm{d}s}{\mathrm{d}t} = r. \tag{2.32}$$

This leads to the following results:

$$r = \frac{c}{2}\left(t^2 + 1\right), \qquad \xi = ct, \qquad \eta = \frac{c}{2}\left(1 - t^2\right). \tag{2.33}$$

Integration of the first equation in (2.2) additionally leads to the new parameter t coinciding (up to a real constant) with the slope angle, i.e.,

$$\theta = t. \tag{2.34}$$

By rewriting Eq. (2.5) in its components, one also has the relations

$$x = \xi \cos t - \eta \sin t, \qquad z = \eta \cos t + \xi \sin t, \tag{2.35}$$

which, combined with the above findings, provides the sought after parameterization of the Sturmian spirals

$$x = c\,(t \cos t + \frac{t^2 - 1}{2} \sin t), \qquad z = c\,(\frac{1 - t^2}{2} \cos t + t \sin t). \tag{2.36}$$

Making use of the above formulas, one also easily finds the arc-length as a function of the parameter t, i.e.,

$$s = \frac{c}{2}(\frac{t^3}{3} + t). \tag{2.37}$$

By exchanging the numerical parameter c for 2ρ and taking into account the fundamental relation $\mathcal{R} \equiv r$ (for this curve), the above formula can be written into the following form, which is none other than the intrinsic equation (in Cesáro form) of the Sturm spiral:

$$s = \frac{(\mathcal{R} + 2\rho)}{3}\sqrt{\frac{\mathcal{R} - \rho}{\rho}}\,. \tag{2.38}$$

2.7 Generalized Sturm Spirals

Due to the restriction on the allowed values of σ, one can also consider the other two obvious possibilities, $\sigma > 1$ and $0 < \sigma < 1$, which have to be viewed as a generalization of the ordinary Sturmian spirals.

2.7.1 The Case When $\sigma > 1$

Here, we will just outline the main ingredients of the derivation, again following the scheme described in Sect. 2.2 starting with the equations

$$\eta = -\sigma r + c \qquad \text{and} \qquad \frac{\mathrm{d}r}{\mathrm{d}s} = \frac{\sqrt{(1 - \sigma^2)r^2 + 2c\sigma r - c^2}}{r}. \tag{2.39}$$

One easily concludes that the expression under the radical on the right-hand side is positive, provided that $c > 0$ and r belongs either to a finite or infinite interval, i.e.,

$$\frac{c}{\sigma + 1} \le r \le \frac{c}{\sigma - 1} \quad \text{and} \quad \sigma > 1 \quad \text{or} \quad r > \frac{c}{\sigma + 1} \quad \text{and} \quad \sigma < 1. \tag{2.40}$$

As the subsection title suggests, our immediate task is to consider the first of the possibilities presented above. Exchanging, as before, the arc-length parameter (cf. Eq. (2.32)) with t, leads to the formula

$$r = \frac{c}{\sigma^2 - 1}(\sigma + \sin\sqrt{\sigma^2 - 1}\, t), \qquad t \in [-\frac{\pi}{2\sqrt{\sigma^2 - 1}}, \frac{\pi}{2\sqrt{\sigma^2 - 1}}], \tag{2.41}$$

by which we also find

$$\xi = \frac{\mathrm{d}r}{\mathrm{d}t} = \frac{c}{\sqrt{\sigma^2 - 1}} \cos\sqrt{\sigma^2 - 1}\, t, \qquad \theta = \sigma\, t. \tag{2.42}$$

The combination of the above results with those from Eq. (2.41), the first equation in (2.39) and the general relations (2.35) gives us

$$\begin{aligned} x &= c\left(\frac{\cos\sqrt{\sigma^2 - 1}\, t\, \cos\sigma t}{\sqrt{\sigma^2 - 1}} + \frac{(\sigma \sin\sqrt{\sigma^2 - 1}\, t + 1)\sin\sigma t}{\sigma^2 - 1}\right) \\ z &= c\left(\frac{\cos\sqrt{\sigma^2 - 1}\, t\, \sin\sigma t}{\sqrt{\sigma^2 - 1}} - \frac{\left(\sigma \sin\sqrt{\sigma^2 - 1}\, t + 1\right)\cos\sigma t}{\sigma^2 - 1}\right). \end{aligned} \tag{2.43}$$

The expressions for the arc-length and the intrinsic equation in this case are

$$s = \frac{c}{\sigma^2 - 1}(\sigma t - \frac{\cos\sqrt{\sigma^2 - 1}\, t}{\sqrt{\sigma^2 - 1}} + \frac{\sigma\pi}{2\sqrt{\sigma^2 - 1}}) \tag{2.44}$$

and

$$\begin{aligned} s = \frac{c}{\sigma^2 - 1}\Bigg(&\frac{\sigma}{\sqrt{\sigma^2 - 1}} \arcsin(\frac{\sigma}{c}\left((\sigma^2 - 1)\mathcal{R} - c\right)) \\ &- \frac{1}{c}\sqrt{\sigma^2(1 - \sigma^2)\mathcal{R}^2 + 2c\sigma^2\mathcal{R} - c^2} + \frac{\sigma\pi}{2\sqrt{\sigma^2 - 1}}\Bigg), \end{aligned} \tag{2.45}$$

where, in the derivation of the last equation, we have used the defining relation for the spiral, which in this case states that $r = \sigma\mathcal{R}$.

A few remarks are in order here. First, while r takes its values in the interval (2.40), the variable t is running in the interval $[-\frac{\sigma\pi}{2\sqrt{\sigma^2-1}}, \frac{\sigma\pi}{2\sqrt{\sigma^2-1}}]$, and during this excursion, the tangent to the curve turns to the angle $\frac{\sigma\pi}{\sqrt{\sigma^2-1}}$. This angle is greater than 2π for $\sigma < \frac{2}{\sqrt{3}}$, equal to 2π for $\sigma = \frac{2}{\sqrt{3}}$ and less than 2π for $\sigma > \frac{2}{\sqrt{3}}$. All this is illustrated in Fig. 2.2.

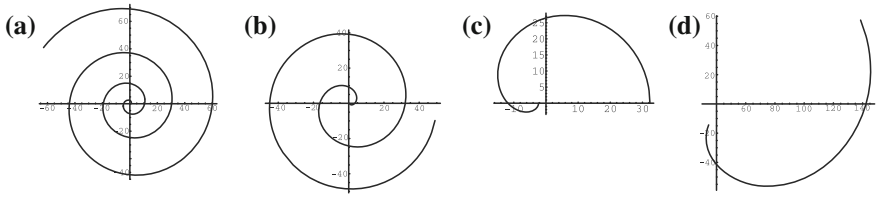

Fig. 2.2 **a** The standard Sturmian spiral generated by (2.36) and $c = 0.25$, and the generalized Sturmian spirals drawn via formulas in (2.43) with the following set of parameters: **b** $c = 1$, $\sigma = 1.02$, **c** $c = 5$, $\sigma = \frac{2}{\sqrt{3}}$, **d** $c = 100$, $\sigma = 5/3$

2.7.2 *The Case When* $0 < \sigma < 1$

The first steps in the scheme amount to

$$\eta = -\sigma r + c, \qquad \frac{\mathrm{d}r}{\mathrm{d}s} = \frac{\sqrt{(1-\sigma^2)r^2 + 2c\sigma r - c^2}}{r}, \tag{2.46}$$

but one should keep in mind that now $\sigma < 1$ and $r > \frac{c}{\sigma+1}$. It also turns out to be more convenient to perform the integration of the equation on the right-hand side in (2.46) by introducing the parameter τ via the equation

$$\frac{\mathrm{d}s}{\mathrm{d}\tau} = r^2, \tag{2.47}$$

which produces

$$r = \frac{c}{\sigma - \sin c\tau}, \qquad \tau \in [-\frac{\pi}{2c}, \frac{\arcsin\sigma}{c}] \tag{2.48}$$

and

$$\begin{aligned} \xi &= -\frac{c\cos c\tau}{\sigma - \sin c\tau}, \qquad \eta = -\frac{c\sin c\tau}{\sigma - \sin c\tau} \\ \theta(\tau) &= \frac{\sigma}{\sqrt{1-\sigma^2}} \ln \frac{\sigma\tan\frac{c\tau}{2} - \sqrt{1-\sigma^2} - 1}{\sigma\tan\frac{c\tau}{2} + \sqrt{1-\sigma^2} - 1}\,. \end{aligned} \tag{2.49}$$

Furthermore, via Eqs. (2.35) and (2.49), we obtain

$$x = \frac{c}{\sigma - \sin c\tau} \cos\left(c\tau - \frac{\sigma}{\sqrt{1-\sigma^2}} \ln \frac{\sigma \tan\frac{c\tau}{2} - \sqrt{1-\sigma^2} - 1}{\sigma \tan\frac{c\tau}{2} + \sqrt{1-\sigma^2} - 1}\right)$$
$$z = \frac{c}{\sigma - \sin c\tau} \sin\left(c\tau - \frac{\sigma}{\sqrt{1-\sigma^2}} \ln \frac{\sigma \tan\frac{c\tau}{2} - \sqrt{1-\sigma^2} - 1}{\sigma \tan\frac{c\tau}{2} + \sqrt{1-\sigma^2} - 1}\right), \tag{2.50}$$

and finally

$$s = \frac{c\sigma}{\left(1-\sigma^2\right)^{3/2}} \ln\left(\frac{\sigma + (1+\sqrt{1-\sigma^2}) \tan\left(\frac{1}{2}\arcsin\left(\frac{c}{r} - \sigma\right)\right)}{1 + \sqrt{1-\sigma^2} + \sigma \tan\left(\frac{1}{2}\arcsin\left(\frac{c}{r} - \sigma\right)\right)}\right) + \frac{\sqrt{(1-\sigma^2)r^2 + 2c\sigma r - c^2}}{1-\sigma^2}. \tag{2.51}$$

As before, one can easily obtain the intrinsic equation of the curve from the last expression by replacing r with $\sigma\mathcal{R}$ (Fig. 2.3).

2.7.3 *The Sub-case When* $0 < \sigma < 1$ *and* $c = 0$

Just for the sake of completeness we will consider the situation when the integration constant c, which appears in the previous subsection, is zero. Obviously, the equations in (2.46) simplify to

$$\eta = -\sigma r, \qquad \frac{\mathrm{d}r}{\mathrm{d}s} = \sqrt{1-\sigma^2}. \tag{2.52}$$

The integration of the second one is immediate and gives us

$$r = \sqrt{1-\sigma^2}\, s + a, \tag{2.53}$$

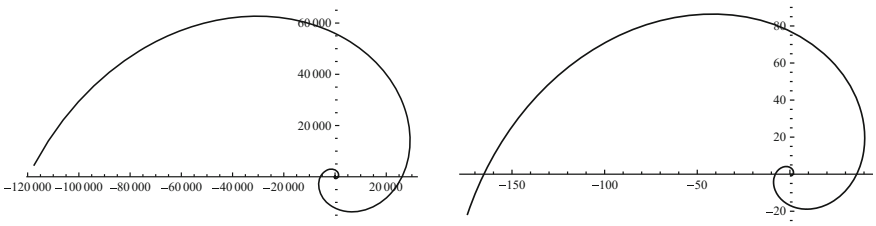

Fig. 2.3 Sturmian spirals generated by formula (2.50) and the constants $\sigma = 0.9$, $c = 1$ (*left*) and formula (2.56) with $\sigma = 0.9$ and $a = 1$ (*right*)

where a denotes a new integration constant that is necessarily positive. Following the scheme, one ends with the results

$$\xi = \left(1-\sigma^2\right)s + a\sqrt{1-\sigma^2}, \qquad \eta = -\sigma\left(\sqrt{1-\sigma^2}\,s + a\right) \tag{2.54}$$

$$\theta(s) = \frac{\sigma}{\sqrt{1-\sigma^2}}\ln(\sqrt{1-\sigma^2}\,s + a), \tag{2.55}$$

which allow us to write down the explicit parameterization of the corresponding spiral

$$\begin{aligned} x &= ((1-\sigma^2)s + a\sqrt{1-\sigma^2})\cos\theta(s) + \sigma(\sqrt{1-\sigma^2}\,s + a)\sin\theta(s) \\ z &= ((1-\sigma^2)s + a\sqrt{1-\sigma^2})\sin\theta(s) - \sigma(\sqrt{1-\sigma^2}\,s + a)\cos\theta(s). \end{aligned} \tag{2.56}$$

Remark It was a challenging task for the present authors (see Mladenov et al. (2011a)) to provide this detailed description from the first principles for the family of Sturm spirals that have such nice geometrical characteristics and to supply their explicit parameterizations. It was kind of a surprise to learn that they do not coincide with any of the famous spirals bearing the names of Archimedes, Cotes, Euler (Cornu), Fermat, Galileo, Nielsens, Poinsot, etc., that are traditionally covered in the textbooks on classical differential geometry (Berger and Gostiaux (1988), Doss-Bachelet et al. (2000), Gray (1998), Oprea (2007) and Rovenski (2000)). Only in the book by Zwikker (1963) was a short note found about the Norwich or Sturm spirals discussed in the previous section. A more thorough search, however, clarifies that the equiangular spiral

$$x = m\,\mathrm{e}^{\phi\cot\alpha}\cos\phi, \qquad z = m\,\mathrm{e}^{\phi\cot\alpha}\sin\phi, \qquad m, \alpha \in \mathbb{R}^+, \quad \phi \in \mathbb{R}, \tag{2.57}$$

discovered by Descartes and sometimes also called a logarithmic spiral, possesses a curvature given by the formula $\kappa = \sin\alpha/r$, and therefore belongs to the class studied in the last two sections. The name of the curve comes from the fact that it cuts the radius vectors from the origin at a constant angle α. This also seems to be the reason behind the fact that insects approach candles along this curve, thinking perhaps that they are flying along a straight line at a constant angle to the rays of the light. Among other interesting properties of this curve, we mention that successive generation of its evolutes, pedal curves or inverses are still equiangular spirals (for more details, see Yates (1959)).

2.8 Serret Curves

A long time ago, Serret (1845) described a family of plane algebraic curves in response to a question raised by Legendre. The problem was to find algebraic curves other than the lemniscate, such that their arc lengths are expressed by elliptic integrals of the first kind. Serret claimed that he had found all such rational curves. Moreover, he provided a mechanical procedure for their construction (Serret (1845a)), which will be described below.

Before that, we will mention that the original Serret curves were indexed by natural numbers, but Liouville (1845) recognized immediately that rational numbers are well-suited enough, as they also lead to algebraic curves. This has been further elucidated in Krohs (1891) dissertation. Here, we extend the definition of Serret's curves from a discrete to a continuous two-parameter family and present their explicit parameterizations. Serret's curves were introduced as a trace of the end point M of the segment OM in the plane XOZ shown in Fig. 2.4.

The lengths of the hinged rods OP and PM are specified by a natural number $n \in \mathbb{N}$ via the formulas $\sqrt{n}$ and $\sqrt{n+1}$, while the point O is fixed at the origin of the Cartesian coordinate system XOZ.

During its movement, the point M describes the curve $\mathcal{S}_n$ according to the rule

$$\cos\omega = \cos(n\alpha - (n+1)\beta), \tag{2.58}$$

where the angles α, β and ω are shown in Fig. 2.4. Their analytical treatment is based on the application of the cosine theorem to the triangle OMP, which gives us

$$\cos\alpha = \frac{r^2-1}{2\sqrt{n}r}, \qquad \cos\beta = \frac{r^2+1}{2\sqrt{n+1}r}. \tag{2.59}$$

Following Liouville's observation, we obtain an algebraic curve even after replacing the index n with the rational number $\nu = p/q$, where $p, q \in \mathbb{N}$. This can be seen to be true by expressing the right-hand side of (2.58) as a polynomial in $\sin\alpha$, $\cos\alpha$, $\sin\beta$ and $\cos\beta$, and then by making use of the geometrical relations (2.59) to obtain the algebraic relations between x and r, and z and r in the form of polynomial equations, i.e.,

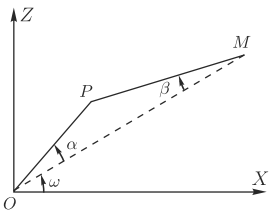

Fig. 2.4 Serret construction

$$P(x, r) = 0, \qquad Q(z, r) = 0. \tag{2.60}$$

Eliminating r between them, one concludes with some polynomial relation

$$F(x, z) = 0, \tag{2.61}$$

and this proves that the curve $\mathcal{S}_\nu$ is algebraic.

We should note that Lipkovski (1996) was recently able to prove that all Serret curves $\mathcal{S}_n$ are rational ones, i.e., they admit rational parameterizations.

Going back to the original Serret (1845a) writings, one can find a formula for the curvature of $\mathcal{S}_n$ in the form

$$\kappa(r) = \frac{3r}{2\sqrt{n(n+1)}} - \frac{2n+1}{2\sqrt{n(n+1)}r}, \tag{2.62}$$

which depends solely on the radial coordinate r. This will be used in the next section to generate them by following the original construction of Mladenov et al. (2010, 2012).

2.8.1 Generalized Serret Curves

The expression for the curvature of Serret's curves (2.62) immediately suggests a generalization of the form

$$\kappa(r) = 3\lambda r - \frac{\sigma}{r}, \qquad \lambda > 0, \qquad \sigma > 1. \tag{2.63}$$

Substitution of (2.63) into (2.8) produces

$$\eta = -\lambda r^3 + \sigma r, \tag{2.64}$$

but one has to notice that the integration constant in (2.8) is taken to be zero. Under these circumstances, the differential equation

$$\dot{r}^2 = \frac{1}{r^2}\left(r^2 - \eta^2\right), \tag{2.65}$$

which follows from (2.9),reduces to the equation

$$\frac{\mathrm{d}r}{\sqrt{(a^2 - r^2)(r^2 - c^2)}} = \lambda \mathrm{d}s, \tag{2.66}$$

in which the real parameters a and c are given by the formulas

$$a = \sqrt{\frac{\sigma + 1}{\lambda}}, \qquad c = \sqrt{\frac{\sigma - 1}{\lambda}}. \tag{2.67}$$

The integration of (2.66) can be performed in terms of the Jacobian elliptic function $\mathrm{dn}(\cdot, \cdot)$, namely,

$$r(s) = a\,\mathrm{dn}(a\lambda s, k), \qquad k = \sqrt{\frac{2}{\sigma + 1}}, \tag{2.68}$$

The next step in the scheme amounts to evaluation of the integral

$$\theta(s) = \int \kappa(r(s))\mathrm{d}s, \tag{2.69}$$

and this gives us

$$\theta(s) = 3\mathrm{am}(\sqrt{\lambda(\sigma + 1)}\, s, k) - \frac{\sigma}{\sqrt{\sigma^2 - 1}} \arccos \frac{\mathrm{cn}(\sqrt{\lambda(\sigma + 1)}\, s, k)}{\mathrm{dn}(\sqrt{\lambda(\sigma + 1)}\, s, k)}, \tag{2.70}$$

where $\mathrm{am}(t, k)$ is the Jacobian amplitude function and $\mathrm{cn}(t, k) = \cos \mathrm{am}(t, k)$.

Having at our disposal (2.7), (2.64), (2.68) and (2.70) can enter into (2.15), giving us the parameterization of the generalized Serret curves. Obviously, the parameterization of the classical Serret curves can be obtained by taking

$$\lambda = \frac{1}{2\sqrt{n(n + 1)}}, \qquad \sigma = \frac{2n + 1}{2\sqrt{n(n + 1)}}, \qquad n \in \mathbb{N}, \tag{2.71}$$

and in this case, the slope angle turns out to be

$$\theta_n(s) = 3\mathrm{am}(\mu_n s, k_n) - (2n + 1) \arccos \frac{\mathrm{cn}(\mu_n s, k_n)}{\mathrm{dn}(\mu_n s, k_n)}, \tag{2.72}$$

where

$$\mu_n = \frac{1}{2}\sqrt{\frac{2\sqrt{n(n + 1)} + 2n + 1}{n(n + 1)}}, \quad k_n = 2\sqrt{\frac{\sqrt{n(n + 1)}}{2\sqrt{n(n + 1)} + 2n + 1}}. \tag{2.73}$$

Several plots of both classical and generalized Serret curves are presented in Fig. 2.5 and Fig. 2.6.

Remark From the viewpoint of curve engineering, the curvature in (2.63) is a superposition of Bernoulli's lemniscate (see Hadzhilazova and Mladenov (2010)) and the Sturmian spiral (Mladenov et al. (2011a)). On the other side, Serret states that the curve $\mathcal{S}_1$ (see Fig. 2.5) coincides with Bernoulli's lemniscate, but looking at the figure, one can see that, besides the lemniscate, there exists an extra part of the curve.

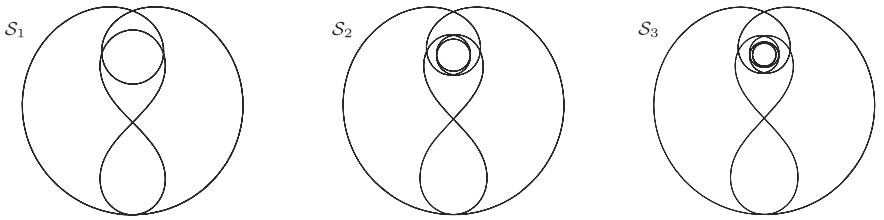

Fig. 2.5 The classical Serret curves $\mathcal{S}_1$ - *left*, $\mathcal{S}_2$ - *middle* and $\mathcal{S}_3$ - *right* for $n = 1, 2, 3$

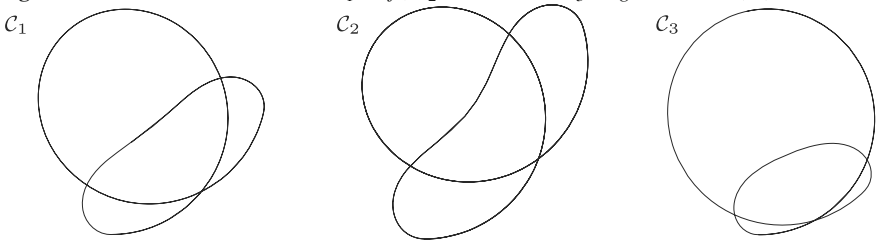

Fig. 2.6 Three examples of the generalized Serret's *curves* $\mathcal{C}_1$ (*left*), $\mathcal{C}_2$ (*middle*) and $\mathcal{C}_3$ (*right*) generated, respectively, with parameter sets $\lambda = 1/3, \sigma = 7/5$, $\lambda = 4/3, \sigma = 9/7$ and $\lambda = 1/7, \sigma = 5/3$

This discrepancy also suggests the necessity of a deeper study of the whole family of Serret curves.

2.9 Cassinian Ovals

This remarkable plane curve is defined as the geometrical locus of the points in the plane for which the product of the distances from two fixed points $\mathbf{F}_1$ and $\mathbf{F}_2$ is a constant, which will be denoted by c^2, and *the distance* $(\mathbf{F}_1, \mathbf{F}_2)$ between $\mathbf{F}_1$ and $\mathbf{F}_2$ is also a constant, denoted by $2a$. In the XOZ plane, the Cassinian ovals are given by the equation (an alternative form is (2.10))

$$(x^2 + z^2 + a^2)^2 - 4a^2x^2 = c^4. \tag{2.74}$$

It is clear that these curves are symmetrical with respect to both coordinate axes. Their shapes depend on the precise relationship of the geometrical parameters a and c. From now on, we will consider the case in which $a < c < a\sqrt{2}$ (this is case *3* in Fig. 2.7). For $c \geqq a\sqrt{2}$, we have ellipse-like figures illustrated by curves numbered as *4* and *5*, and when $c = a$, the curve is given by the equation

$$(x^2 + z^2)^2 = 2a^2(x^2 - z^2), \tag{2.75}$$

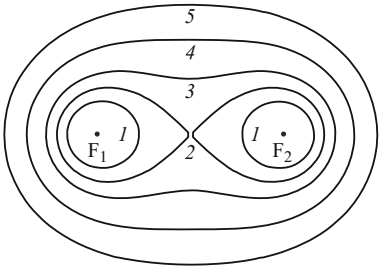

Fig. 2.7 Cassinian ovals drawn with different values of dimensionless ratio $\varepsilon = a/c$

which is nothing less than the Bernoullian lemniscate reproduced here as curve *2*. Finally, in the case in which $a > c$, the curves reduce to two disjoint ovals (these ovals are depicted as curves *1* in Fig. 2.7).

Cassini has proposed the fourth degree curves (2.74) in an attempt to describe the planetary motions in the solar system properly. Equations (2.74) and (2.75) describe concrete algebraic curves. The meaning of the last notion is that the rectangular coordinates x, z of the points on the curve C in the plane satisfy an algebraic equation

$$F(x, z) = 0, \tag{2.76}$$

where $F(x, z)$ is a polynomial function in its variables.

Following the tradition established by Canham (1970), Deuling and Helfrich (1976), Funaki (1955) and Vayo (1983), the Cassinian ovals can be considered as a model of red blood cells. For more detail, see Angelov and Mladenov (2000) and Hadzhilazova et al. (2011).

2.9.1 Alternative Parameterizations

By making use of the general formula for the curvature of curves defined implicitly as $F(x, z) = 0$, i.e.,

$$\kappa(x, z) = \frac{|F_{xx}F_z^2 - 2F_{xz}F_xF_z + F_{zz}F_x^2|}{(F_x^2 + F_z^2)^{3/2}}\,{}_{|F=0}, \tag{2.77}$$

one can easily find that the curvature of the Cassinian ovals (2.74) is given by the formula

$$\kappa(r) = \frac{a^4 - c^4}{2c^2r^3} + \frac{3r}{2c^2}. \tag{2.78}$$

This formula makes clear the fact that the curvature is a function depending only on the polar radius r (as the parameters a and c are considered to be fixed).

2.9.1.1 Integration

Here, we will present a scheme (see Hadzhilazova et al. (2011)), by which one can reconstruct (in principle) any plane curves whose curvature depends solely on the distance from the origin, i.e., $\kappa \equiv \kappa(r)$. For this purpose, let us recall the general formula for the curvature in polar coordinates (see (1.16))

$$\kappa = \frac{r^2 + 2\dot{r}^2 - r\ddot{r}}{(r^2 + \dot{r}^2)^{3/2}}, \tag{2.79}$$

where the dots over r denote the derivatives with respect to the polar angle ϕ. The introduction of the new variable

$$\dot{r} = \frac{\mathrm{d}r}{\mathrm{d}\phi} = \tau \tag{2.80}$$

has, as a result, the useful formula

$$\phi = \int \frac{\mathrm{d}r}{\tau}\cdot \tag{2.81}$$

We also have

$$\ddot{r} = \frac{\mathrm{d}^2 r}{\mathrm{d}\phi^2} = \frac{\mathrm{d}\dot{r}}{\mathrm{d}\phi} = \frac{\mathrm{d}\tau}{\mathrm{d}\phi} = \frac{\mathrm{d}\tau}{\mathrm{d}r}\frac{\mathrm{d}r}{\mathrm{d}\phi} = \tau\frac{\mathrm{d}\tau}{\mathrm{d}r}, \tag{2.82}$$

and therefore

$$\kappa = \frac{r^2 + 2\tau^2 - r\tau\frac{\mathrm{d}\tau}{\mathrm{d}r}}{(r^2 + \tau^2)^{3/2}} = \frac{2}{(r^2 + \tau^2)^{1/2}} - \frac{r^2 + r\tau\frac{\mathrm{d}\tau}{\mathrm{d}r}}{(r^2 + \tau^2)^{3/2}}\cdot \tag{2.83}$$

The above formulas also suggest introduction of the notation

$$r^2 = \xi, \qquad r^2 + \tau^2 = \zeta \tag{2.84}$$

and, making use of them, the possibility of writing

$$r^2 + r\tau\frac{\mathrm{d}\tau}{\mathrm{d}r} = \xi\frac{\mathrm{d}\zeta}{\mathrm{d}\xi}, \tag{2.85}$$

which ultimately leads to the formula

$$\kappa(\xi) = \frac{2}{\sqrt{\zeta}} - \frac{\xi}{\sqrt{\zeta^3}}\frac{\mathrm{d}\zeta}{\mathrm{d}\xi} = 2\frac{\mathrm{d}}{\mathrm{d}\xi}\left(\frac{\xi}{\sqrt{\zeta}}\right)\cdot \tag{2.86}$$

The integration of the last equation gives us

$$\frac{\xi}{\sqrt{\zeta}} = \frac{1}{2}\int \kappa(\xi)\mathrm{d}\xi. \tag{2.87}$$

Going back to the original coordinates, one ends up with the equation

$$\frac{r^2}{\sqrt{r^2+\tau^2}} = \int r\kappa(r)\mathrm{d}r. \tag{2.88}$$

Performing the integration on the right-hand side produces

$$\int r\kappa(r)\mathrm{d}r = m(r) - \omega, \tag{2.89}$$

where ω denotes the integration constant. Solving the system of Eqs. (2.88) and (2.89) for τ, one gets

$$\tau = \frac{r\sqrt{r^2-(m(r)-\omega)^2}}{m(r)-\omega} \tag{2.90}$$

and, respectively,

$$\phi = \int \frac{m(r)-\omega}{r\sqrt{r^2-(m(r)-\omega)^2}}\,\mathrm{d}r, \tag{2.91}$$

which is the result that will be used extensively in what follows. Here, the integration constant is omitted, as it is responsible only for the choice of the polar axis, which can be done arbitrarily.

In order to obtain concrete results, one has to specify the curvature in explicit form, which we will do below.

2.9.1.2 Parameterization

The result for the Cassinian oval (2.78), suggests consideration of the curves whose curvature is given by the general formula

$$\kappa = \frac{\lambda}{r^3} + \mu r = \frac{\lambda}{r^3} + 3\nu r, \qquad \lambda \in \mathbb{R}, \quad \nu \in \mathbb{R}^+. \tag{2.92}$$

In what follows, we will present the parametric equations of the curves whose curvature is specified in (2.92) using the method just described. It is easy to see that strongly positive values of the parameters λ and μ exactly reproduce the Cassinian oval due to the relations

$$a^4 = \frac{4\lambda\mu+1}{4\mu^2}, \qquad c^2 = \frac{1}{2\mu}. \tag{2.93}$$

The above range of parameters could be easily extended by adding negative values of λ which fulfill, together with μ, the inequality

$$4\lambda\mu + 1 > 0. \tag{2.94}$$

Further on, this will be taken for granted, but let us mention that it also includes some negative values of λ, which means that the corresponding curves should actually be considered as a deformation (Mladenov et al. (2011)) of the parent curve (2.78).

Applying formulas (2.89) and (2.91) with (2.92) produces, respectively,

$$m(r) = -\frac{\lambda}{r} + \nu r^3 \tag{2.95}$$

and

$$\phi = \nu \int \frac{r^3 \mathrm{d}r}{\sqrt{-\nu^2 r^8 + (2\lambda\nu + 1)r^4 - \lambda^2}} - \lambda \int \frac{\mathrm{d}r}{r\sqrt{-\nu^2 r^8 + (2\lambda\nu + 1)r^4 - \lambda^2}}.$$

The above integrals can be uniformized by the following chain of substitutions:

$$r^2 = \chi = n\,\mathrm{dn}(u, k), \qquad n = \frac{\sqrt{2\,\lambda\,\nu + 1 + \sqrt{4\,\lambda\,\nu + 1}}}{\sqrt{2}\,\nu}, \tag{2.96}$$

where $\mathrm{dn}(u, k)$ is one of the Jacobian elliptic functions, u is the uniformizing parameter and

$$k = \sqrt{\frac{2\sqrt{4\,\lambda\,\nu + 1}}{2\,\lambda\,\nu + 1 + \sqrt{4\,\lambda\,\nu + 1}}}$$

is the elliptic modulus. As a result, the integrals for the polar angle transform into

$$\phi = \frac{1}{2}\left(\frac{\lambda}{\nu n^2 \tilde{k}} \int \frac{\mathrm{d}u}{\mathrm{dn}(u, k)} - \int \mathrm{dn}(u, k)\mathrm{d}u\right), \quad \tilde{k} = \sqrt{\frac{2\,\lambda\,\nu + 1 - \sqrt{4\,\lambda\,\nu + 1}}{2\,\lambda\,\nu + 1 + \sqrt{4\,\lambda\,\nu + 1}}}$$

and can then be evaluated, i.e.,

$$\phi(u) = \frac{1}{2}\left(\frac{\lambda}{\nu n^2 \tilde{k}} \arccos \frac{\mathrm{cn}(u, k)}{\mathrm{dn}(u, k)} - \mathrm{am}(u, k)\right), \tag{2.97}$$

where $\mathrm{am}(u, k)$ is the Jacobian amplitude function and $\mathrm{cn}(u, k) = \cos \mathrm{am}(u, k)$.

Alternatively, the integrals defining the polar angle ϕ can be evaluated via the substitution $r^4 = t$, and as a result, this gives us

$$\phi(r) = \frac{1}{4}\left(\arcsin \frac{2\,\nu^2\,r^4 - 2\,\lambda\,\nu - 1}{\sqrt{4\,\lambda\,\nu + 1}} + \arcsin \frac{2\,\lambda^2 - (2\,\lambda\,\nu + 1)\,r^4}{\sqrt{4\,\lambda\,\nu + 1}\,r^4}\right). \tag{2.98}$$

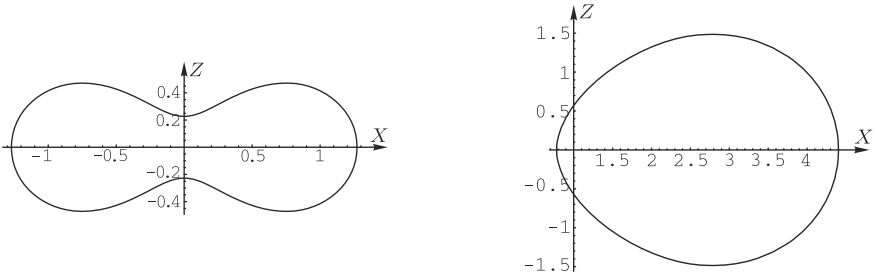

Fig. 2.8 The biconcave *curve* on the *left-hand side* is produced via (2.97) with parameters $\lambda = -0.05$ and $\nu = 0.6$. The internal *oval* on the *right-hand side* is generated via (2.98) with $\lambda = -0.59$ and $\nu = 0.05$

Remark Let us point out that the above parameterizations are entirely different from those reported in Mladenov (2000), Mladenov et al. (2011) and Angelov and Mladenov (2000). Besides, one should note a subtle difference between the formulas (2.97) and (2.98)– the first one is capable of producing both external and internal Cassinian ovals, but not the Bernoullian lemniscate (see Hadzhilazova and Mladenov (2010)), while the second one can be used to draw the lemniscate and the internal ovals, but omits the biconcave curves (see Figs. 2.7 and 2.8).

References

B. Angelov, I. Mladenov, On the geometry of red blood cells. Geom. Integr. Quant. **1**, 27–46 (2000)
M. Berger, B. Gostiaux, *Differential Geometry: Manifolds Curves and Surfaces* (Springer, New York, 1988)
B. Canham, The minimum energy of bending as a possible explanation of biconcave shape of the human red blood cell. J. Theoret. Biol. **26**, 61–81 (1970)
H. Deuling, W. Helfrich, Red blood cell shapes as explained on the basis of curvature elasticity. Biophys. J. **16**, 861–868 (1976)
P. Djondjorov, M. Hadzhilazova, I. Mladenov, V. Vassilev, A note on the passage from the free to the elastica with a tension. Geom. Integr. Quant. **10**, 175–182 (2009)
P. Djondjorov, V. Vassilev, I. Mladenov, Plane curves associated with integrable dynamical systems of the Frenet-Serret type, in *9th International Workshop on Complex Structures, Integrability and Vector Fields*, ed. by K. Sekigawa, V. Gerdjikov, S. Dimiev (World Scientific, Singapore, 2009a), pp. 56–62
C. Doss-Bachelet, J.-P. Françoise, C. Piquet, *Géométrie differentielle* (Ellipses, Paris, 2000)
H. Funaki, Contribution on the shapes of red blood corpuscles. Japan J. Physiol. **5**, 81–92 (1955)
A. Gray, *Modern Differential Geometry of Curves and Surfaces with Mathematica®*, 2nd edn. (CRC Press, Boca Raton, 1998)
M. Hadzhilazova, I. Mladenov, On Bernoulli's lemniscate and co-lemniscate. CRAS (Sofia) **63**, 843–848 (2010)
M. Hadzhilazova, I. Mladenov, Once more the mylar balloon. CRAS (Sofia) **61**, 847–856 (2008)
M. Hadzhilazova, I. Mladenov, P. Djondjorov, V. Vassilev, New parameterizations of the Cassinian ovals. Geom. Integr. Quant. **12**, 164–170 (2011)
E. Jahnke, F. Emde, F. Lösch, *Tafeln Höherer Funktionen* (Teubner, Stuttgart, 1960)

G. Krohs, Die Serret'schen Kurven sind die einzigen algebraischen vom Geschlecht Null, deren Koordinaten eindeutige doppelperiodische Functionen des Bogens der Kurve sind. Inaugural Dissertation Halle-Wittenberg Universität 74 p. (1891)
J. Liouville, A note on the Serret's article. J. Mathematiques Pures et Appliquées **10**, 293–296 (1845)
A. Lipkovski, Serret's curves, in *Book of Abstracts of the International Topological Conference Topology and Applications*, 191–192 Phasis, Moscow (1996)
S. Matsutani, Euler's elastica and beyond. J. Geom. Symmetry Phys. **17**, 45–86 (2010)
I. Mladenov, Uniformization of the Cassinian oval. CRAS (Sofia) **53**, 13–16 (2000)
I. Mladenov, M. Hadzhilazova, P. Djondjorov, V. Vassilev, On some deformations of the Cassinian oval, in *AIP Conference Proceedings* vol 1340, (New York 2011) pp 81–89
I. Mladenov, M. Hadzhilazova, P. Djondjorov, V. Vassilev, On the plane curves whose curvature depends on the distance from the origin, in *AIP Conference Proceedings*, vol. 1307 (New York, 2010), pp. 112–118
I. Mladenov, J. Oprea, Balloons, domes and geometry. J. Geom. Symmetry Phys. **15**, 53–88 (2009)
I. Mladenov, M. Hadzhilazova, P. Djondjorov, V. Vassilev, On the generalized Sturmian spirals. C. R. Bulg. Acad. Sci. **64**, 633–640 (2011a)
I. Mladenov, M. Hadzhilazova, P. Djondjorov, V. Vassilev, Serret's curves, their generalization and explicit parametrization, in *Geometric Methods in Physics*, ed. by P. Kielanowski, S.T. Ali, A. Odzijewicz, M. Schlichenmaier, Th Voronov (Basel, Birkhäuser, 2012), pp. 383–390
F. Olver, D. Lozier, R. Boisvert, Ch. Clark (eds.), *NIST Handbook of Mathematical Functions* (Cambridge Univ. Press, Cambridge, 2010)
J. Oprea, *Differential Geometry and Its Applications*, 3rd edn. (Mathematical Association of America, Washington D. C, 2007)
V. Rovenski, *Geometry of Curves and Surfaces with Maple®* (Birkhäuser, Boston, 2000)
J.-A. Serret, Sur la représentation géometrique des fonctions elliptiques et ultra-elliptiques. J. Mathematiques Pures et Appliquées **10**, 257–290 (1845)
J.-A. Serret, Sur les courbes elliptiques de la première classe. J. Mathematiques Pures et Appliquées **10**, 421–429 (1845a)
D. Singer, Curves whose curvature depends on distance from the origin. Am. Math. Monthly **106**, 835–841 (1999)
V. Vassilev, P. Djonjorov, I. Mladenov, Integrable dynamical systems of the Frenet-Serret type, in *Proceeding 9th International Workshop on Complex Structures, Integrability and Vector Fields*, ed. by K. Sekigawa, V. Gerdjikov, S. Dimiev (World Scientific, Singapore, 2009) pp. 234–244
H. Vayo, Some red blood cell geometry. Can. J. Physiol. Pharmacol. **61**, 646–649 (1983)
R. Yates, *Curves and Their Properties* (Edwards Brothers, Ann Arbor, 1959)
C. Zwikker, *The Advanced Geometry of Plane Curves and Their Applications* (Dover, New York, 1963)

http://www.springer.com/978-3-319-61242-3

The Many Faces of Elastica

Mladenov, I.M.; Hadzhilazova, M.

2017, XV, 212 p. 85 illus., 6 illus. in color., Hardcover
ISBN: 978-3-319-61242-3